Model for Variable-Length Electrical Arc Plasmas Under AC Conditions

Ziran Wu, Guichu Wu, Marcelo Dapino, Lezhen Pan, and Kan Ni

***Abstract*— This paper proposes a mathematical model for electrical discharge plasmas between moving electrodes under ac condition, which happens in ac switching apparatuses. The modeling work is started by converting the problem to a conventional *RL* network that treats the arcing phenomenon as a black box and proposing a transient differential equation to represent the breaking arc process. A resistance–time relation model developed from the classic Mayr model is then proposed. A conceptual unit-arc approach is used to deal with the issue of variable arc length as the contacts move. Experimental data from ac contactor tests are used to approximate the resistance–time function by a nonlinear curve fitting. The model is solved computationally and compared with the experimental data. It is that the model adequately describes the breaking arc phenomenon.**

***Index Terms*— Arc discharges, curve fitting, modeling.**

I. Introduction

THIS paper focuses on mathematical modeling on electrical arcs, or termed electrical discharges, between a pair of moving electrodes with alternating currents (ac). The issue is raised as this type of arcs commonly occurs in ac switching apparatuses during breaking processes. In this paper, the switching apparatuses investigated work in low voltage and normal temperature and there was air between contacts (differing from the vacuum types). The proposed work differs from most other plasma researches by investigating nonconstant length plasmas as well as combining behaviors of arc plasmas and electrical circuits.

A breaking arc plasma consists of ionized air and a vaporized metal, and as such, it generates a large amount of heat and light. The arc starts just at the moment when the two contacts begin to separate. The air between the contacts is ionized and the ions move from one of the electrodes, through the gap and into the other. Therefore, macroscopically after the contact separation, the current will remain for a short duration. That is how a breaking arc plasma is being generated. The arc usually quenches when the ac current reaches zero. Meanwhile, the body of the arc moves to the arc chamber that helps to extinguish the arc. The process of an arc typically takes several milliseconds. Since an arc plasma generates a great amount of heat within a small region, the local temperature increases very quickly and the central temperature can rise to over 5000 K [1], [2]. The high temperature erodes and melts the contacts. Thus, the arcing phenomenon is the key factor that influences the electrical durability of apparatuses. Therefore, this paper aims to improve the understanding of breaking arc plasmas via mathematical modeling, while also contributing to the practical design of electrical apparatuses.

Manuscript received March 7, 2015; revised May 24, 2015; accepted June 23, 2015. Date of publication July 27, 2015; date of current version August 7, 2015. This work was supported by the Zhejiang Provincial Key Science and Technology Innovation Team through the Project entitled Low-Voltage Apparatus Technologies for Smart Grids under Project 2010R50006.

Z. Wu, G. Wu, and K. Ni are with the Key Laboratory of Low-Voltage Apparatus Intellectual Technology of Zhejiang, Wenzhou University, Wenzhou 325027, China (e-mail: nature.nano@gmail.com; wgc@wzu.edu.cn; nikankind2@gmail.com).

M. Dapino is with the Department of Mechanical and Aerospace Engineering, The Ohio State University, Columbus, OH 43210 USA (e-mail: dapino.1@osu.edu).

L. Pan is with Wenzhou Power Supply Company of State Grid, Wenzhou 325604, China (e-mail: lenapun@163.com).

Color versions of one or more of the figures in this paper are available online at http://ieeexplore.ieee.org.

Digital Object Identifier 10.1109/TPS.2015.2450214

II. Prior Work

A. Review

Generally speaking, there are two ways to describe arc plasmas. One is to investigate, simulate, and represent the particle behaviors of an arc, i.e., behaviors of atoms and electrons, and so usually arcs are measured by optical, acoustic, or thermal sensors [3]–[5]. This type of approach studies the details within the arcing region. However, errors of these sensors are significant when they measure an arc within a very short duration. The temperature of an arc can only be approximately estimated using the intensity of luminance or sound from an optical or acoustic sensor. On the other hand, the response speed of a thermal sensor is not fast enough to trace the variation of the arc temperature.

The other way to describe arc plasmas is to represent an important electrical characteristic—electrical conductance variation with time. Black box models [6] are the most common approach, which treats the arc as a black box relating electrical conductance and arc energy. It has been argued that the thermal energy is the key factor that keeps an arc blazing so that the conductance can be reflected by thermal balance (assuming that the energy of the arc is associated with the thermal balance). The classic Mayr arc model [7] (it is in German, and [8] and [9] illustrate the theory in English), was derived by estimating the energy balance during the arcing duration. The model is represented by an ordinary differential equation (ODE) that assumes the cooling power is constant. This equation is suitable for low-current arcs ($\leq$500 A) [8]. The Cassie model [10] is similar to the Mayr model. It assumes that the temperature inside the zone of an arc is constant in both space and time, and then involves a constant parameter—the arc reference voltage drop—to represent energy dissipation. This model is suitable for relatively high-current arcs ($\geq$500 A).

Researchers developed models from the Mayr and Cassie models by addressing some (but not all) complexities of arc formation and decay. Schwarz [11] incorporated the conductance into the thermal balance representation. The Habedank model [12], the KEMA model [13], as well as a model proposed in [14] discuss that arcs cannot be simply described by a single conductance–energy model. These models treat an arc as a series of subarcs, and each subarc can be represented by a Mayr or Cassie model.

B. Discussion on Moving Electrodes

However, the approaches introduced above are not well suited for the arc type investigated in this paper. The key reason is that moving electrodes lead to a variable length of each arc plasma. Therefore, it is inappropriate to consider the cooling factors for the Mayr or Cassie model to be constant. In addition, there is little evidence to support the Cassie model in that the arc temperature is unchanged in the time domain between two electrodes [8].

Garzon [15] discussed the ac issue and referred a number of models describing the breaking arc phenomenon in electrical switching apparatuses, especially a model proposed in [16]. The model combines thermal dynamics of arcs with electrical signals and discusses the changed arc length. However, it does not focus on the effect of arc length variation, which significantly influences heat density and dissipation of arcs.

To solve the *variable-length issue*, this paper introduces an approach that segments an arc into a series of several *unit arcs* that have a unit length. According to Ohm's law, the resistance of the arc is the sum of the *unit arc* resistances. Then an arc can be treated as a variable resistor and integrated into a circuit topology. The detail will be discussed in the following sections.

III. Breaking Arc Model

A. Base Model

In the research, the maximum rated current is limited up to 480 A, which matches the condition of the Mayr model. The Mayr model assumes that the impedance of an arc can be considered resistive, and the conductivity or resistivity is uniform within the arcing zone. The conductance g can be represented by

$$g = k \cdot e^{\frac{Q}{Q_0}}$$

where k and Q_0 are constant, and Q denotes the stored energy. According to this formula, when the stored energy Q drops to zero, the conductance g is equal to k. In practice, however, g is supposed to be zero when the stored energy is zero. To solve this contradiction, denote the power generated by the arc by P_{in} and the dissipation power by P_{out}, so that the equation is altered to

$$g = k \cdot \left(e^{\frac{Q}{Q_0}} - 1\right) = k \cdot \left(e^{\frac{1}{Q_0}\int (P_{\text{in}} - P_{\text{out}})dt} - 1\right). \quad (1)$$

Then the equation can be transformed to a logarithmic differential form like the standard Mayr equation

$$\frac{\ln g}{dt} = \frac{1}{g}\frac{dg}{dt} = \frac{e^{\frac{Q}{Q_0}}}{e^{\frac{Q}{Q_0}} - 1}\frac{P_{\text{out}}}{Q_0}\left(\frac{P_{\text{in}}}{P_{\text{out}}} - 1\right).$$

When Q/Q_0 is relatively large, the first fraction can be approximated to 1. Meanwhile, if P_{out} is constant as assumed in the Mayr model, the above equation is equivalent to the standard Mayr equation. Alternatively, for resistance one obtains

$$R = \frac{1}{g} = \frac{k}{e^{\frac{Q}{Q_0}} - 1} = \frac{k}{e^{\frac{1}{Q_0}\int (P_{\text{in}} - P_{\text{out}})dt} - 1}. \quad (2)$$

B. Hypotheses

For a breaking arc between a contact pair, we follow the Mayr model to assume the following.

1) The shape of the arc is approximated cylindrical, which is the same approximation made by [16].
2) The heat is uniformly distributed along the cylindrical zone. Therefore, the arc temperature is constant in space within the arcing zone but varies in time during the breaking process.
3) The representations of the arc conductance and resistance are represented by (1) and (2), respectively.
4) Unlike Mayr's hypotheses, the cooling power is not constant but linearly related to the length of the cylindrical arcing zone

$$P_{\text{out}} = k_1 \cdot D(t). \quad (3)$$

5) When the two contacts are closed, the contact resistance between them is approximated to zero. Therefore, the resistance during the breaking process is completely caused by the arc.

C. Model Topology

An experimental electrical circuit that simulates realistic application conditions is built. The topology of the circuit can be simplified as a pair of moving electrodes that connects to an inductor and a resistor in series, and an ac power source is applied, which is shown in Fig. 1.

The inductance L and resistance r are the constants that can be measured or computed directly. When the electrodes are firmly closed, its impedance can be approximated to 0. When it is completely open, the impedance is infinity. When it is breaking (opening) with an arc blazing, the impedance can be treated as a time-dependent resistance denoted $R(t)$. The ac power source is a conventional sine function

$$u(t) = U_0 \cdot \sin(\omega t + \theta)$$

where θ is the phase difference between the voltage and current. The power factor is defined as $\text{PF} = |\cos(\theta)|$. Denoting the current $i(t)$, a breaking process can be indicated by a transient ODE

$$\frac{d}{dt}i(t)L + [r + R(t)] \cdot i(t) = u(t) = U_0 \cdot \sin(\omega t + \theta). \quad (4)$$

According to [17], the solution of (4) is

$$i(t) = e^{-A(t)}\left[\int \frac{U_0 \cdot \sin(\omega t + \theta)}{L} e^{A(t)}dt + \kappa_0\right] \quad (5)$$

$$A(t) = \int \frac{r + R(t)}{L}dt = \frac{r}{L}t + \int \frac{R(t)}{L}dt + C.$$

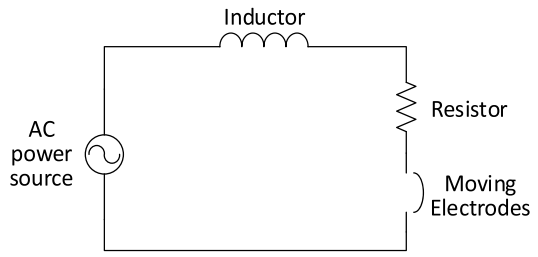

Fig. 1. Model topology.

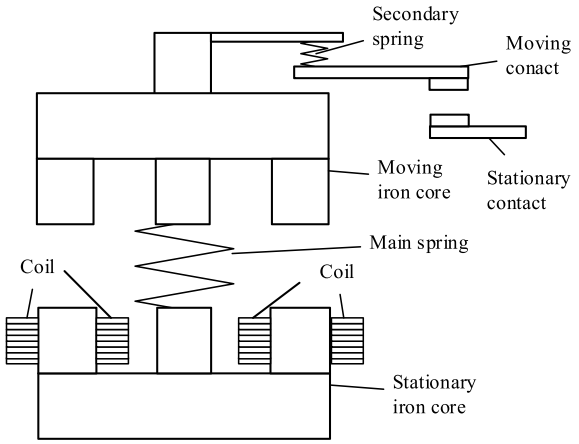

Fig. 2. Structure of the ac contactor.

The integral constant κ_0 can be worked out by the initial electrical condition of the breaking process. The problem is that this was reduced to finding the resistance of the arc $R(t)$. However, as discussed in Section II, the arc phenomenon of a breaking process is very complicated, and cannot be approximated by any conventional theoretical models. We solve this problem by performing nonlinear regression on experimental data.

D. Electrode Motion Description

In the experiment, a type of ac contactors is used as arc plasma generators. Fig. 2 indicates the structure of the ac contactor. The moving and stationary contacts is connected to the main circuit. The coils are driven by a 220 V voltage. In a close (make) process, when current flows via the coils, the stationary iron core is magnetized. The moving iron coil is pulled toward the stationary one by the magnetic suction, and meanwhile drives the moving contact to move down until reaching the stationary contact. While in an open (break) process, whence the main circuit is switched OFF, the current via the coils is cut off and there is no suction between the iron cores. The main spring forces the iron coils moving farther and the contacts begin to separate and the main circuited is switched OFF. Since there is still current remaining through the two contacts, an arc plasma occurs between the two contacts.

According to the structure and mechanism of the ac contactors, the arc length equals the distance between a pair of contacts (electrodes). Hypothesis 4 (see the hypotheses in Section III-B) describes a method to calculate the dissipation power by the displacement of the moving contact. To investigate the movement of a moving contact in breaking processes, we measure the displacement values of the moving contact in a number of breaking operations. Four typical examples are shown in Fig. 3. Fig. 3(a) indicates two experimental results of contact movements of a brand new ac contactor, while Fig. 3(b) indicates another two experimental results of contact displacements of an ac contactor having operated 6014 times.

We have carried out 10 breaking processes for both the brand new and the operated ac contactors. All measurement results are similar to what is represented in Fig. 3. It can be noted that there are two inflections (A and B) in each curve: the inflection A represents the beginning of the contact disconnection, while inflection B indicates the moving contact being stopped. The bounces after inflection point B are not the focus of this paper. From Fig. 2, by neglecting the impulses that are caused by measurement errors, it can be observed that on each curve the relation between inflections A and B is approximately linear. Therefore, from the beginning of the contact disconnection to the stop of the moving contact, the movement of the moving contact is considered a uniform displacement at constant speed.

The measurements are explained as follows. The breaking process starts, the magnetic force from the coil becomes zero, and the main springs force the iron core to move with the contacts still connected. When the iron core has moved farther than the overtravel distance, the main springs no longer produce repulsive force and the iron core pulls the moving contact to leave the stationary one by inertia. Since the mass of the iron core is much larger than the contact, the acceleration duration is very short (inflection A) and the iron core and the contact reach a status of uniform motion quickly. Then before the contact being stopped, it receives almost no resistance force, so the motion is approximately uniform. Finally, the contact is stopped (inflection B) and bounces happen.

According to Fig. 3, there is no significant difference between the uniform motion durations of the brand new and aged ac contactors. The uniform motion durations are approximately 9 ms, while according to the data from breaking tests, generally an arc keeps blazing for a duration shorter than a half electrical period (10 ms). References [18] and [19] study the same ac contactor type with this paper and illustrate that actually the duration of an arc is shorter than 9 ms. Therefore, the distance between the contacts $D(t)$ is proportional to time t with a constant factor k_2 and an initial distance of zero

$$D(t) = k_2 \cdot t. \tag{6}$$

E. Arc Resistance Description

We apply (1) to approximate the arc resistance as a function of time. Now the problem is how to achieve the stored energy Q in (1). Assuming that the arc starts at time t_0 and using Hypotheses 3 and 4, the stored energy at time t is ($t > t_0$)

$$\begin{aligned} Q &= \int [u(t)i(t) - k_1 D(t - t_0)]dt \\ &= \int u(t)i(t)dt - \int k_1 k_2 (t - t_0)dt \\ &= \int u(t)i(t)dt - c \cdot \int (t - t_0)dt \end{aligned} \tag{7}$$

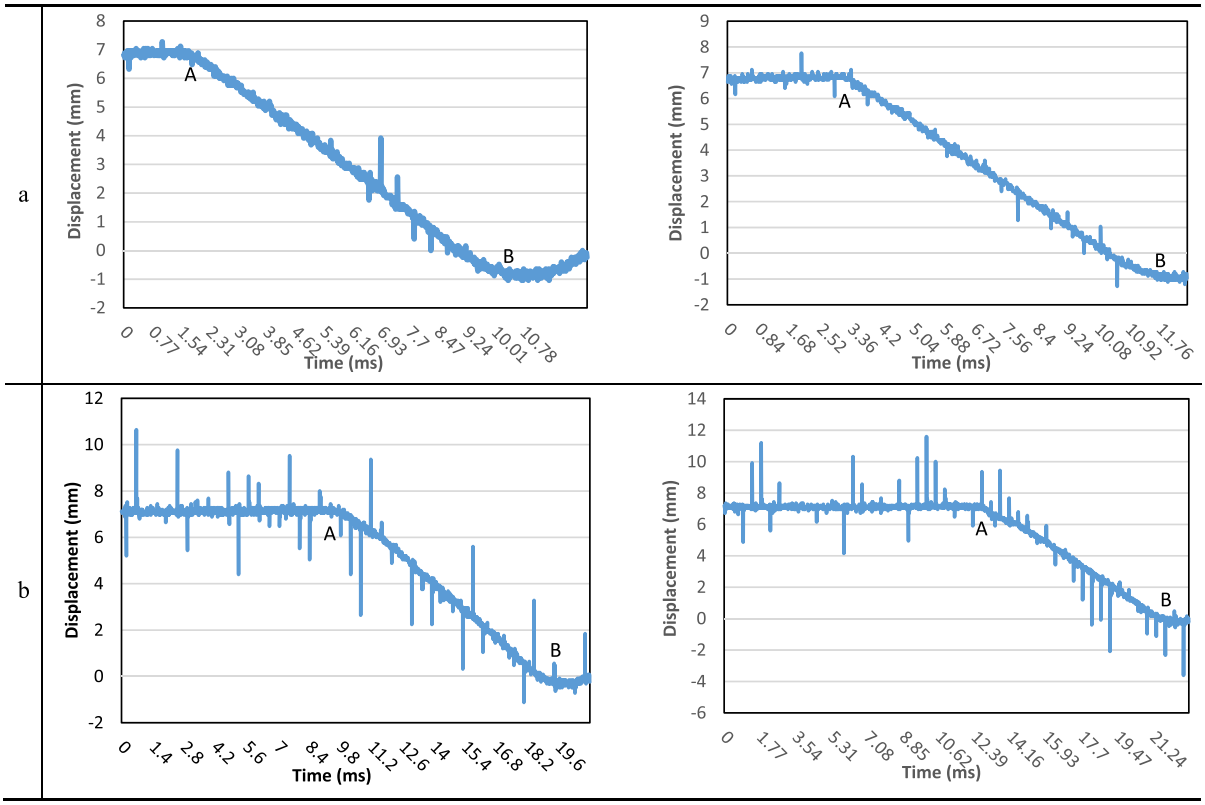

Fig. 3. Displacement of the moving contact. (a) Contact breaking displacements of a brand new AC contactor. (b) Contact breaking displacements of an aged AC contactor.

where c is a nonnegative constant. At the beginning of the breaking process, the initial stored energy is zero, so the integral constant is zero. To solve the *variable-length issue*, we define a subarc whose length is a unit distance as a *unit arc*. According to Hypothesis 1, the stored energy per distance unit is $Q/D(t-t_0)$. Combining with (1), one obtains the resistance per distance unit

$$R_{\text{unit}}(t) = \frac{k_4}{e^{k_3 Q/D(t-t_0)} - 1} = \frac{k_4}{e^{\frac{b}{t-t_0}\int [u(t)i(t) - c\cdot(t-t_0)]dt} - 1} \tag{8}$$

where k_3, k_4, and b are all constant, and $b > 0$. Then according to Hypothesis 1 and Ohm's law, the arc resistance can be considered a series resistance of several *unit arcs*

$$\begin{aligned} R(t) &= R_{\text{unit}}(t)D(t-t_0) \\ &= \frac{a\cdot(t-t_0)}{e^{\frac{b}{t-t_0}\int [u(t)i(t) - c\cdot(t-t_0)]dt} - 1} (t > t_0) \end{aligned} \tag{9}$$

where a is a merged constant by k_2 and k_4.

F. Equation Solution

Let

$$B(t) = \frac{r}{L}t + \int \frac{R(t)}{L}dt.$$

Apply it to (5) to eliminate the constant

$$\begin{aligned} i(t) &= \frac{U_0}{L}\cdot e^{-B(t)-C}\left[\int \sin(\omega t+\theta)\cdot e^{B(t)+C}dt + \kappa_0\right] \\ &= \frac{U_0}{L}\cdot e^{-B(t)}\left[\int \sin(\omega t+\theta)\cdot e^{B(t)}dt + \kappa\right] \end{aligned} \tag{10}$$

where $\kappa = \kappa/e^C$, which is also a constant and can be worked out by the initial electrical condition of the breaking process. Assuming that the arc starts at time t_0, the time transient before t_0 is t_{0-} while that after is t_{0+}, according to Hypothesis 5, it can be obtained that

$$R(t_{0-}) = R(t_{0+}) = 0.$$

In an inductive circuit, the current does not change in a transient duration, that is to say

$$i(t_{0+}) = i(t_{0-}).$$

Then represent the transient current just before and after t_0

$$\begin{aligned} i(t_{0-}) &= I_0\sin(\omega t_0) \\ &= \frac{U_0\sin(\omega t_0)}{\sqrt{(R(t_{0-})+r)^2 + (\omega L)^2}} = \frac{U_0\sin(\omega t_0)}{\sqrt{r^2+(\omega L)^2}} \\ i(t_{0+}) &= \frac{U_0}{L}\cdot e^{-\frac{r}{L}t_0 - \int_{t_0}^{t_{0+}}\frac{R(y)}{L}dy} \\ &\quad\times\left[\int_{t_0}^{t_{0+}} \sin(\omega t+\theta)\cdot e^{\frac{r}{L}t + \int_{t_0}^{t}\frac{R(y)}{L}dy}dy + \kappa\right] \\ &= \kappa\cdot\frac{U_0}{L}\cdot e^{-\frac{r}{L}t_0}. \end{aligned}$$

The outcome of any definite integral from t_0 to t_{0+} is zero. Therefore, finally, κ is derived as

$$\kappa = \frac{L\cdot\sin(\omega t_0)\cdot e^{\frac{r}{L}t_0}}{\sqrt{r^2+(\omega L)^2}}. \tag{11}$$

TABLE I
CONTACTOR SPECIFICATION AND TEST CONFIGURATION

Parameter	Value
AC contactor maximum rated current	80 A
Voltage on the coil	220 V
Line voltage	380 V
Phase voltage	220 V
Electricity frequency	50 Hz
AC-4 rated current	480 A
Sampling rate	30,000 Hz

TABLE II
IMPEDANCE CONFIGURATION OF THE LOAD SET

Impedance	Phase		
	A	B	C
Resistance (Ω)	0.1514	0.1676	0.1838
Inductance (mH)	1.1139	1.0542	1.0744

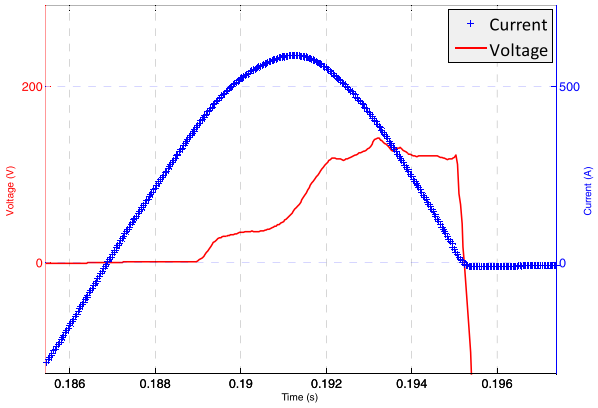

Fig. 4. Waveform of a breaking process.

IV. NUMERICALLY COMPUTATIONAL VERIFICATION

A. Data Acquisition

We verify the model by comparing the current waveforms computed by the model with the measured current waveforms occur during breaking processes in AC-4 tests [20]. The data used in our numerically computational verification are acquired by an ac contactor testing and acquisition system. The contactor specification and the AC-4 test configuration are shown in Tables I and II, and a data example is shown in Fig. 4.

In Table II, the resistance and inductance are the parameters r and L in the equations, respectively, and vary between phases due to the structure of the load set. In (9), the voltage and current functions $u(t)$ and $i(t)$ are required. However, according to the electrical signals acquired in the tests, $u(t)$ is not a derivable function (see Fig. 4). Therefore, a mathematical representation of $u(t)$ as well as $i(t)$ is very difficult. Thus, the resistance can only be obtained by numerical computation. According to Fig. 4, the arcing duration starts from the moment when the voltage rises, and ends at the moment when the current reaches zero. However, in some conditions, arcs continue blazing after the current crosses zero, and do not quench until the next zero-crossing [18]. Considering that this condition rarely happens in a well-designed and qualified ac contactor, it will not be discussed in this paper.

B. Verification Procedure

So far, numerically verification cannot be performed since there are a number of unknown parameters in the proposed model. To estimate the values of a, b, and c in (9), we perform nonlinear curve fitting on multiple sets of data acquired from a number of breaking processes. Now a problem is addressed: one of the arcing characteristics—the arcing phase angle—significantly influents arc behaviors [18], [19]. An arc phase angle (APA) indicates where an arc starts within an ac period. Reference [18] illustrates how to compute arcing phase angles (termed arcing phases in [18]). Hence, we separate the arc data by their APAs, and each curve fitting process aims at arcs with the same APA. During a curve fitting process, the following constraint conditions are applied.

1) The resistance of an arc is nonnegative, so $a > 0$.
2) The dissipation power $P_{\text{out}} = c \cdot (t - t_0)$ is nonnegative. Since $t > t_0$, it is implicitly assumed that $c > 0$.
3) The stored energy Q must be nonnegative, so during the breaking process, it must be guaranteed that

$$Q(t) = \int_{t_0}^{t} [u(t)i(t) - c \cdot (t - t_0)]dt > 0.$$

4) The conductance g will increase when the stored energy Q rises. Since $t > t_0$ and $Q > 0$, according to (2) and (9), it can be obtained that $b > 0$.

Similarly, it is very difficult to work out the mathematical expression of the integral in (10). However, numerical computation can be performed to achieve integral values. Therefore, for numerical computation, (10) can be transformed to (12), and the results are shown in Fig. 5

$$\begin{aligned} i(t) &= \frac{U_0}{L} \cdot e^{-\frac{r}{L}t - \int_{t_0}^{t} \frac{R(y)}{L} dy} \\ &\quad \times \left[\int_{t_0}^{t} \sin(\omega x + \theta) \cdot e^{\frac{r}{L}t + \int_{t_0}^{x} \frac{R(y)}{L} dy} dx + \kappa \right] \\ &= \frac{U_0}{L} \cdot e^{-\frac{r}{L}t - \int_{t_0}^{t} \frac{a \cdot (y - t_0)}{L \cdot (e^{\frac{b}{y - t_0} \int_{t_0}^{y} [u(z)i(z) - c \cdot (z - t_0)]dz} - 1)} dy} \\ &\quad \cdot \left[\int_{t_0}^{t} \sin(\omega x + \theta) \right. \\ &\quad \left. \cdot e^{\frac{r}{L}x + \int_{t_0}^{x} \frac{a \cdot (y - t_0)}{L \cdot (e^{\frac{b}{y - t_0} \int_{t_0}^{y} [u(z)i(z) - c \cdot (z - t_0)]dz} - 1)} dy} dx + \kappa \right]. \end{aligned} \quad (12)$$

Hence, finally, the procedure of the numerical computational verification for the proposed model can summarized as follows.

1) Experimental waveforms of the same APA are collected as a set. For each waveform, the corresponding resistance curve of the arc is computed (see Fig. 5, Row A).
2) All resistance curves of the same APA are applied to achieve the parameters in (9) (a, b, and c), by performing curve-fitting. The voltage and current data [$u(t)$ and $i(t)$] used in (9) is from the corresponding waveform (see Fig. 5, Rows B and C).
3) The achieved resistance parameters (a, b, and c) are applied to (12), so all parameters in (12) are known and $i(t)$ for each breaking arc can be computed (see Fig. 5, Row D).

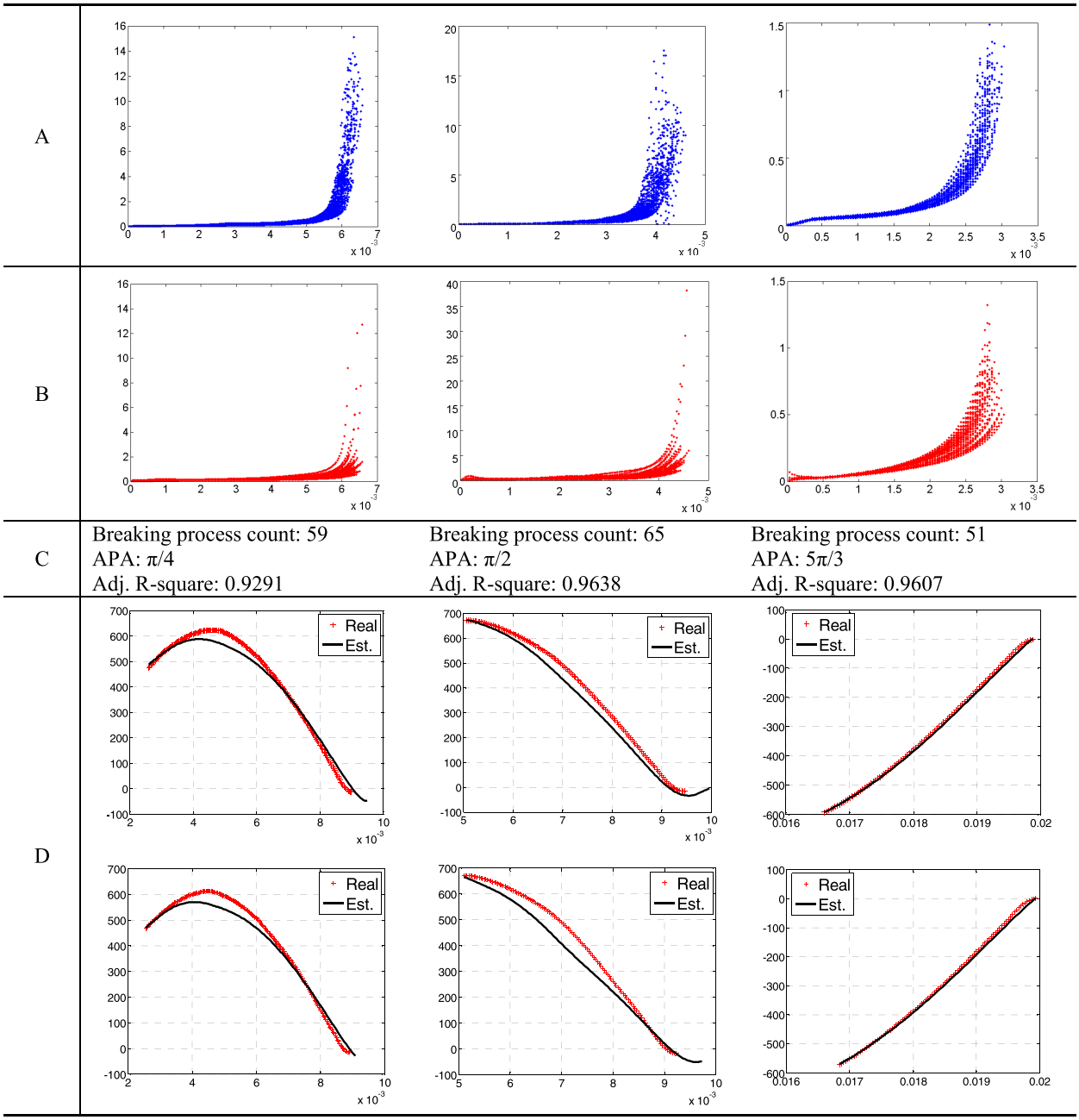

Fig. 5. Results of computational verification. A—measured resistance: y-axis: resistance (Ω) and x-axis: time (s). B—resistance computed by curve fitting: y-axis: resistance (Ω) and x-axis: time (s). C—fitting information. D—comparison between the measured and calculated waveforms: y-axis: current (A) and x-axis: time (s).

C. Results and Discussion

The fitting results of three APAs are shown in Fig. 5, Rows A and B. All of the curve fitting processes achieve adjusted R-square [21] values over 0.9. Row A of Fig. 5 indicates three examples of measured resistance values calculated directly from the acquired voltage and current data, while Row B of Fig. 5 exhibits the computed resistance values that achieved by applying fitted a, b, and c to (9). The fitting information is displayed in Row C of Fig. 5. It is observed that the computed resistance can approximate the measured data. However, compared with the computed resistance curves, the measured resistance curves are more compact in the earlier period and increase faster in the later period.

We calculate the integral by the adaptive Simpson quadrature [22] and then estimate the current. Fig. 5, Row D shows three examples of the estimated current (Est.) waveforms compared with the measured ones (Real). The APAs of these examples correspond to Rows A and B in Fig. 5. It can be observed that the estimated current waveforms are very close to the measured ones. For the left and the middle columns of Fig. 5, the estimated curves are slightly lower than the measured ones, which means the model produces larger suppression on the current than the reality. However, the starting and zero-crossing timings of the estimated curves and the measured ones are very close. For the right column, the estimated and measured curves are almost overlapped, which

means that the model is well fitted to the arcing condition. Meanwhile, an interesting phenomenon can be observed in Fig. 5: when reaching zero, each of the measured currents continues to vary to a small opposite value, and then slowly approaches zero. It can also be observed that the estimated current curves are able to represent the continued variation the zero crossings. Hence, in summary, the proposed model is able to represent the breaking arc phenomenon of ac contactors.

V. Conclusion

This paper advances the Mayr model to describe arc plasmas between moving contacts under ac conditions. A number of hypotheses are made to approximate the arcing process. *Unit arcs* are used to deal with the *variable-length issue*. Data from AC-4 tests on ac contactors are used to estimate the parameters by nonlinear curve fitting and numerically verify the representibility of the model. The computational results show that the model can achieve a relatively high accuracy to describe the arc phenomenon.

Future work will focus on conducting additional tests and estimating the model parameters with different APAs. Then the relations between the parameters and the APAs are expected to be worked out so that the mathematical arc model will be associated with the APA. Meanwhile, although the experiments are based on ac contactors, it can be extend the modeling method to other types of switching apparatus, such as relays and circuit breakers, on which the modeling work will be more difficult since the arc length variation will be nonlinear upon time.

Acknowledgment

The work was completed by the Key Laboratory of Low-voltage Apparatus Intellectual Technology of Zhejiang, Wenzhou University. Meanwhile, the authors would like to thank the Quality Supervision, Inspection and Quarantine Bureau of Wenzhou as well as the National Industrial Quality Supervision and Inspection Center, which contributed to the work by providing a large quantity of testing data.

References

[1] M. Takeuchi and T. Kubono, "A spectroscopic detecting system for measuring the temperature distribution of silver breaking arc using a CCD color camera," *IEEE Trans. Instrum. Meas.*, vol. 48, no. 3, pp. 678–683, Jun. 1999.

[2] T. Kitajima, J. Sekikawa, M. Takeuchi, and T. Kubono, "Temperature measurements of breaking arc between copper contacts at three constant speeds (10, 20 and 30 mm/s)," *IEICE Trans. Electron.*, vols. E87-C, no. 8, pp. 1361–1366, Aug. 2004.

[3] M. I. Al-Amayreh, H. Hofmann, O. Nilsson, C. Weindl, and A. R. Delgado, "Arc movement inside an AC/DC circuit breaker working with a novel method of arc guiding: Part II—Optical imaging method and numerical analysis," *IEEE Trans. Plasma Sci.*, vol. 40, no. 8, pp. 2035–2044, Aug. 2012.

[4] P. Teste, T. Leblanc, J. Rossignol, and R. Andlauer, "Contribution to the assessment of the power balance at the electrodes of an electric arc in air," *Plasma Sour. Sci. Technol.*, vol. 17, no. 3, p. 035001, May 2008.

[5] Y. Wu, M. Rong, Z. Sun, X. Wang, F. Yang, and X. Li, "Numerical analysis of arc plasma behaviour during contact opening process in low-voltage switching device," *J. Phys. D, Appl. Phys.*, vol. 40, no. 3, pp. 795–802, 2007.

[6] A. Balestrero, L. Ghezzi, M. Popov, G. Tribulato, and L. van der Sluis, "Black box modeling of low-voltage circuit breakers," *IEEE Trans. Power Del.*, vol. 25, no. 4, pp. 2481–2488, Oct. 2010.

[7] O. Mayr, "Beitrage zur theorie des statischen und des dynamischen lichtbogens," *Arch. Elektrotechn.*, vol. 37, no. 12, pp. 588–608, 1943.

[8] L. Ghezzi and A. Balestrero, "Modeling and simulation of low voltage arcs," Ph.D. dissertation, Dept. Elect. Sustain. Energy, Delft Univ. Technol., Delft, The Netherlands, Oct. 2010.

[9] P. Schavemaker and L. van der Slui, "An improved Mayr-type arc model based on current-zero measurements [circuit breakers]," *IEEE Trans. Power Del.*, vol. 15, no. 2, pp. 580–584, Apr. 2000.

[10] A. M. Cassie, "Arc rupture and circuit severity," CIGRE, Paris, France, Tech. Rep. 102, 1939.

[11] J. Schwarz, "Dynamisches verhalten eines gasbeblasenen, turbulenzbestimmten schaltlichtbogens," *ETZ Arch.*, vol. 92, pp. 389–391, 1971.

[12] U. Habedank, "Application of a new arc model for the evaluation of short-circuit breaking tests," *IEEE Trans. Power Del.*, vol. 8, no. 4, pp. 1921–1925, Oct. 1993.

[13] R. P. P. Smeets and V. Kertesz, "Evaluation of high-voltage circuit breaker performance with a validated arc model," *IEE Proc.-Generat., Transmiss. Distrib.*, vol. 147, no. 2, pp. 121–125, Mar. 2000.

[14] J. L. Guardado, S. G. Maximov, E. Melgoza, J. L. Naredo, and P. Moreno, "An improved arc model before current zero based on the combined Mayr and Cassie arc models," *IEEE Trans. Power Del.*, vol. 20, no. 1, pp. 138–142, Jan. 2005.

[15] R. D. Garzon, *High Voltage Circuit Breakers: Design and Applications*, 2nd ed. New York, NY, USA: Marcel Dekker, 2002.

[16] W. Hermann and K. Ragaller, "Theoretical description of the current interruption in HV gas blast breakers," *IEEE Trans. Power App. Syst.*, vol. 96, no. 5, pp. 1546–1555, Sep. 1997.

[17] J. C. Robinson, *An Introduction to Ordinary Differential Equations*. Cambridge, U.K.: Cambridge Univ. Press, 2004.

[18] Z. Wu, Y. You, G. Wu, and H. Huang, "Research on arcing characteristics of AC contactor breaking processes based on statistics," in *Proc. 5th Int. Conf. Rel. Elect. Products Elect. Contacts*, Nov. 2014, pp. 70–75.

[19] Z. Wu, G. Wu, H. Huang, and Y. You, "A novel residual electrical endurance prediction method for low-voltage electromagnetic alternating current contactors," *IEEE Trans. Compon., Packag., Manuf. Technol.*, vol. 5, no. 4, pp. 465–473, Apr. 2015.

[20] *Low-Voltage Switchgear and Controlgear*, IEC Standard 60947, Jan. 2007.

[21] H. Theil, *Economic Forecasts and Policy*. Amsterdam, The Netherlands: North Holland, 1961.

[22] W. Gander and W. Gautschi, "Adaptive quadrature—Revisited," *BIT Numer. Math.*, vol. 40, no. 1, pp. 84–101, 2000.

Ziran Wu was born in 1984. He received the Ph.D. degree from the University of York, York, U.K., in 2013.

He is currently a Research Associate with the Key Laboratory of Low-Voltage Apparatus Intellectual Technology of Zhejiang, Wenzhou University, Wenzhou, China. His current research interests include data analysis on electrical apparatus, including arc modeling, reliability, endurance prediction, fault detection, electric automatization and intellectualization, including applications of automatic and intelligent manufacturing, and industrial image processing.

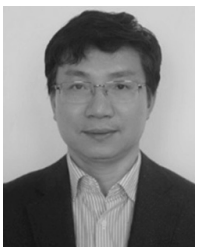

Guichu Wu is currently the Director of the Key Laboratory of Low-Voltage Apparatus Intellectual Technology of Zhejiang with Wenzhou University, Wenzhou, China, where he is a Professor with the College of Physics and Electronic Information Engineering. He is the Director of Zhejiang Technology Service Platform of Wenzhou Low-Voltage Apparatus. His current research interests include electric intellectualization, embedded system applications, and solar energy.

Prof. Wu is also a Committee Member of the International Conference on Reliability of Electrical Products and Electrical Contacts.

Marcelo Dapino is currently the Honda R&D Americas Designated Chair of Engineering with The Ohio State University, Columbus, OH, USA, where he is a Professor with the Department of Mechanical and Aerospace Engineering. He serves as Director of the Honda-OSU Mobility Innovation Exchange, as an Associate Director for Research of the Smart Vehicle Concepts Center and the National Science Foundation Industry/University Cooperative Research Center, and is also a Senior Fellow of the Ohio State University Center for Automotive Research. His current research interests include design and manufacture of smart material systems.

Prof. Dapino is also a member of the Executive Committee of the American Society of Mechanical Engineers Aerospace Division, and has led the organization of major American Society of Mechanical Engineers and the Society for Optical Engineering Conferences.

Lezhen Pan was born in 1984. She received the B.S. degree from the School of Electrical Engineering, Zhejiang University, Hangzhou, China, in 2007, and the M.Sc. degree from the School of Electrical Engineering, Shanghai Jiao Tong University, Shanghai, China, in 2010.

She is currently an Engineer with Wenzhou Power Supply Company of State Grid, Wenzhou, China. Her current research interests include reliability of electrical equipment and power supply, and power system planning.

Kan Ni is currently pursuing the master's degree in low-voltage apparatus intellectualization with the Key Laboratory of Low-Voltage Apparatus Intellectual Technology of Zhejiang, Wenzhou University, Wenzhou, China.

He is also a Research Member of the Key Laboratory of Low-Voltage Apparatus Intellectual Technology of Zhejiang with Wenzhou University. His current research interests include electrical arcs and relevant reliability issues, life-cycle-simulation using finite element method, and arc fault semiphysical simulation.